JOURNAL OF THERMOPHYSICS AND HEAT TRANSFER
Vol. 21, No. 4, October–December 2007

Thermal Modeling for the Sustained Hypersonic Flight Experiment

Jenny S. Goodman* and Peter T. Ireland†
Oxford University, Oxford, OX1 3PJ England, United Kingdom

DOI: 10.2514/1.29317

This paper details the development, validation, and use of a thermal model created to predict the surface temperatures through the U.K. Ministry of Defence funded sustained hypersonic flight experiment ramjet vehicle. The sustained hypersonic flight experiment ramjet will operate at Mach 4 to 6 leading to very high airflow stagnation temperatures. It was therefore important to predict the temperatures during the flight experiment at an early design stage, before the vehicle geometry was finalized and before detailed computer-aided design models were available. The heat exchange mechanisms throughout the acceleration section of the sustained hypersonic flight experiment were predicted using a thermal resistance network incorporating convection, radiation, and conduction. The flexibility of the model allowed sustained hypersonic flight experiment Mach 4 combustion ground experiment thermal systems to be predicted using the same methodology as the flight experiment thermal model. The predicted ground experiment combustor exit temperatures showed good agreement with the measured experimental temperatures, providing confidence in the thermal modeling technique. The sustained hypersonic flight experiment thermal modeling technique was also used to aid the design of the ground experiment cooling water system, assess the reliability of thermocouple measurements, and analyze the suitability of a range of flameholder designs.

Nomenclature

A	=	area, m^2
C	=	circumference, m
C_p	=	specific heat at constant pressure, $J \cdot kg^{-1} \cdot K^{-1}$
C^*	=	characteristic velocity, $m \cdot s^{-1}$
H	=	heat transfer coefficient, $W \cdot m^{-2} \cdot K^{-1}$
h	=	static enthalpy, $J \cdot kg^{-1}$
h_0	=	total enthalpy, $J \cdot kg^{-1}$
k	=	thermal conductivity, $W \cdot m^{-1} \cdot K^{-1}$
m	=	mass of single segment of C/SiC outer tube, kg
Pr	=	Prandtl number
P_0	=	total pressure, $N \cdot m^{-2}$
Q	=	heat input rate per unit of air mass flow, W
R	=	thermal resistance
R_c	=	gas constant per unit weight, $J \cdot K^{-1} \cdot kg^{-1}$
Re	=	Reynolds number
r	=	radius, m
St	=	Stanton number
T	=	static temperature, K
T_0	=	total temperature, K
U	=	velocity, $m \cdot s^{-1}$
x	=	axial distance from combustor entrance

Subscripts

aw	=	adiabatic wall
axial	=	axial conduction
c	=	combustion chamber
cond	=	conduction
conv	=	convection
DS	=	downstream model section
f	=	fuel
g	=	combustion gas
i	=	inner surface
j	=	jacket
net	=	net heat flow
o	=	outer surface
rad	=	radiation
t	=	titanium
US	=	upstream model section
w	=	water
x	=	axial distance from combustor entrance, m
z	=	zirconia insulation
∞	=	main flow property

Symbols

ℓ	=	thermal model section length, m
γ	=	specific heat ratio
Δ	=	change in property
ε	=	emissivity
μ	=	dynamic viscosity, $kg \cdot m^{-2} \cdot K^{-1}$
ρ	=	density, $kg \cdot m^{-3}$
σ	=	Stephan–Boltzmann constant, 5.68×10^{-8} $W \cdot m^{-2} \cdot K^{-1}$
$*$	=	reference property

I. Introduction

THE objective of the U.K. Ministry of Defence (MOD) funded sustained hypersonic flight experiment (SHyFE) is to design and fly a prototype ramjet engine capable of sustained hypersonic flight [1]. After release from a rocket booster the SHyFE vehicle will accelerate from Mach 4 to Mach 6 where it will cruise for a specified range. Figure 1 shows the internal layout of the SHyFE vehicle. Air enters the annular combustion chamber at subsonic speeds and diesel or JP10 fuel is injected through two rings of 12 swirl injectors. A flameholder is located downstream of the rear injector to improve the SHyFE combustion efficiency and to aid the fuel autoignition. The final SHyFE vehicle will be mainly constructed from carbon/silicon carbide (C/SiC), with the gap between the centerbody and outer wall maintained by eight struts close to the intake lip and the flameholder located in the combustion chamber. The centerbody is a titanium tank containing pressurized gas and fuel and the outer wall

Presented as Paper 8071 at the 14th AIAA/AHI International Space Planes and Hypersonic Systems and Technologies Conference, Canberra, Australia, 6–9 November 2006; received 15 December 2006; revision received 18 March 2007; accepted for publication 27 March 2007.

*Doctor of Philosophy Student, Engineering Science, Parks Road. Student Member AIAA.
†Professor of Engineering Science, Parks Road.

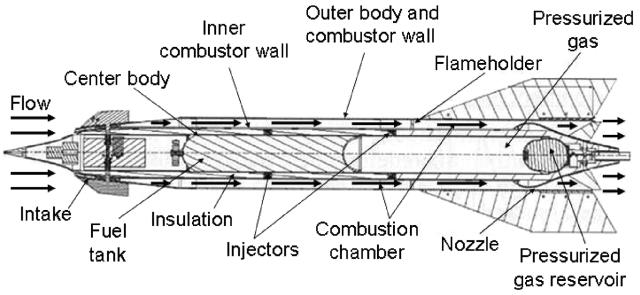

Fig. 1 Cross section of the SHyFE vehicle [16].

of the combustion chamber and nozzle is also the cowl of the SHyFE vehicle. C/SiC has been selected for the SHyFE vehicle construction because it can maintain 300 MPa strength up to 2350 K [2]. The use of C/SiC allows the SHyFE surfaces to be passively cooled by radiating to the surroundings, simplifying the thermal design and reducing the weight of the vehicle. The centerbody contains the flight control actuators and computer and therefore the gap between the combustion chamber and the centerbody is filled with 12 mm of zirconia felt insulation [3] to help maintain these temperature sensitive components within their operating range. To aid the design of the SHyFE vehicle, a thermal model was produced to predict the nozzle surface temperatures and heat flow during the acceleration section of the final flight experiment. This was designed to provide a quick and flexible assessment of the vehicle temperatures and heat flows.

The thermal model did not require finite element modeling to determine the heat and temperature distribution, allowing design changes to be easily assessed. This flexibility allowed the model to be validated using data from Mach 4 SHyFE combustion ground experiments, as these experiments were assessed using the same methodology as for the combustion chamber and nozzle during flight. The validation was undertaken by comparing the predicted combustor exit gas temperature at a range of equivalence ratios against the temperatures measured during the SHyFE experiment. The thermal model also aided the Mach 4 combustion experiment's cooling water system design and was used to assess the validity of the combustor internal wall thermocouple measurements.

II. Overview of Thermal Modeling

A series of steady-state thermal models were developed to assess the SHyFE combustion chamber and nozzle surface temperatures during the final flight experiments and Mach 4 combustion ground tests. The thermal models were based on a network of thermal resistance equations which describe the flow of heat through the nozzle and combustion chamber annular layers. An iteration procedure was employed to ensure that the heat flow from the combustion and nozzle gases into the resistance network equalled the heat flow leaving the resistance network at the outer surface of the vehicle and through axial conduction along the combustion chamber and nozzle walls. The flight thermal model was also used to assess the temperature increase associated with a range of flameholder designs. This analysis was undertaken at Mach 4 flight conditions using heat transfer coefficients downstream of the flameholders derived from experiments performed by the authors and detailed in [4].

The SHyFE during flight thermal model methodology was also used to predict the temperatures through two SHyFE Mach 4 combustion ground experiments performed by QinetiQ, the prime contractor company for the SHyFE project. The Mach 4 combustion experiment containing C/SiC combustor walls with zirconia insulation between the inner combustion chamber and nozzle surface and the centerbody was used to validate the flight thermal model. Infrared temperature sensors (pyrometers) were used in QinetiQ's experiments to measure the external combustor outer surface and thermocouples measured the external inner combustor wall temperature. The authors' thermal model was also used to assess the thermocouple measurements during the Mach 4 combustion experiment containing zirconia insulation between the combustor and the centerbody. The design of an alternative Mach 4 combustion experiment containing an air gap between the combustor and centerbody was also aided by using the thermal model to predict the surface temperatures through the experiment.

III. Thermal Modeling of SHyFE Combustion Chamber and Nozzle During Flight

During the SHyFE flight experiment a rocket booster will be used to accelerate the SHyFE vehicle to Mach 4 at 15 km altitude. At this point the ramjet will be released from the booster and will climb under its own power to 32 km while accelerating from Mach 4 to 6. The acceleration will be followed by approximately 100 s of constant altitude Mach 6 cruise, until all the fuel has been burned and the vehicle falls to Earth [1].

A thermal model was developed to calculate the combustion chamber and nozzle surface temperatures and heat flow during the acceleration stage of the SHyFE mission. This allowed the temperatures of the combustor walls, fuel tank, actuators, and flight control computer to be assessed, to ensure that the thermal limit of the components would not be exceeded. The thermal model of the SHyFE combustion chamber and nozzle during flight also enabled the temperature and heat flow increases associated with a range of flameholder designs to be analyzed.

A. SHyFE Combustion Chamber and Nozzle During Flight Thermal Model Configuration

Figures 2a and 2b show the geometry and nomenclature used for the combustion chamber and nozzle during flight. The walls are constructed from C/SiC with a layer of zirconia insulation located between the centerbody and the combustor and nozzle inner walls. The centerbody is a titanium tank containing pressurized gas and fuel and the outer wall of the combustor and nozzle is also the cowl of the SHyFE vehicle. The model therefore calculated the properties of the external air at the appropriate Mach number and altitude during the SHyFE acceleration, so that the temperature and heat transfer coefficient for the external flow could be predicted.

B. SHyFE Combustion Chamber and Nozzle During Flight Model Methodology

The temperatures and heat flow through the SHyFE combustion chamber and nozzle were calculated for the acceleration section of the SHyFE flight using combustion gas and external air predictions provided by QinetiQ. The internal and external gas temperatures

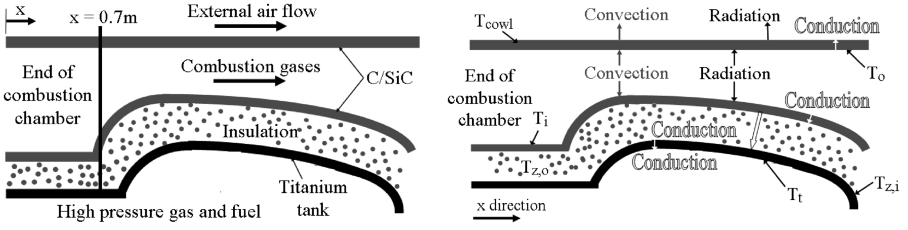

a) Configuration **b) Heat flow and Nomenclature**

Fig. 2 SHyFE combustion chamber and nozzle during flight model configuration.

were supplied for 47 time points during the flight, separated by 1.5 s intervals. The calculation procedure was a steady-state analysis, meaning that the temperatures along each short segment of the combustor and nozzle were assumed to remain constant throughout each 1.5 s time period of the SHyFE acceleration, and energy was not stored within the combustor and nozzle walls. Therefore heat flowing from the combustor into each short section of the model combustion chamber or nozzle was balanced with the heat flowing into the atmosphere via radiation and convection and axially along the vehicle through the process of axial conduction. The heat flow into the nozzle and combustor walls was caused by the high temperature gases transferring some of their thermal energy through convection to the combustor walls; this energy was then transmitted radially through the model surfaces by conduction, radiation, and convection.

The steady-state analysis was considered to provide a good prediction of the SHyFE temperatures and heat flows during flight if heat transfer equilibrium was reached by the end of each time segment. This was investigated using a simplified transient heat transfer model to calculate the time required for steady-state heat transfer to occur in a number of segments and time periods. The transient model included the heat storage term shown in Eq. (1), where m is the mass of a single segment of C/SiC outer tube and C_p is the specific heat at constant pressure for C/SiC. The conduction and radiation heat flow into the combustion chamber outer wall and from the combustion chamber outer wall to the external air were calculated using the same equations as the full steady-state thermal model, described in Sec. III.B.2. H and the wall starting temperatures were also obtained using the full SHyFE during flight steady-state thermal model. The transient heat transfer model calculated the combustion chamber exit wall temperatures at 0.01 s intervals, so that the time for steady-state conditions to be produced through the SHyFE vehicle could be analyzed.

$$\text{Energy stored} = m \cdot C_p \cdot \Delta T \tag{1}$$

Steady-state conditions were assumed to have occurred when the heat energy stored by the combustor wall reduced to 2% of the heat transfer supplied to the outer combustor wall and the wall temperature changed by less than 0.5% s^{-1}. Using appropriate values of C_p, emissivity ε, and ρ for the SHyFE C/SiC walls [5], it was found that steady-state heat transfer could be obtained within 1.5 s if the SHyFE thermal model combustion chamber and nozzle was split into 1257, 0.0007 m length sections. Figure 3 shows the heat stored and supplied to the outer combustor wall, calculated using the transient thermal model for the first 2.4 s of the SHyFE acceleration. By analyzing a number of time points through the SHyFE acceleration, the time for steady-state conditions to occur was found to lie between 1 and 1.5 s depending on the gas properties during each time point of the SHyFE acceleration. It was therefore concluded that the temperatures and heat transfer predicted by the full steady-state thermal model would be pessimistic at the beginning, but correct by the end of each time segment.

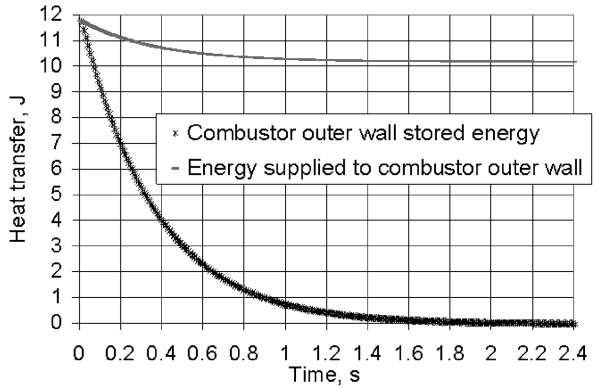

Fig. 3 Transient thermal model prediction of heat supplied to and stored in combustor outer wall during the first 2.4 s of SHyFE acceleration.

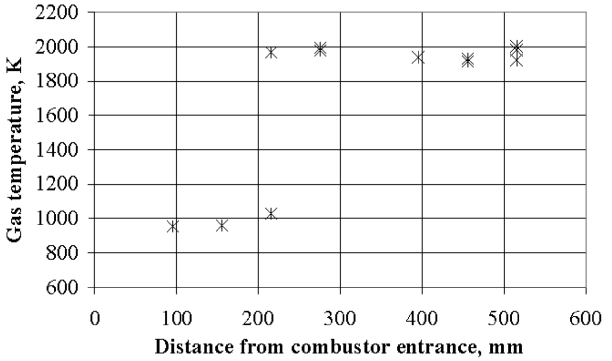

Fig. 4 Gas temperature calculated using the thermal model along the combustion chamber for the SHyFE Mach 4 C/SiC combustion experiment.

1. Gas and External Air Property Calculations

Figure 4 shows the gas temperatures calculated using the thermal model during the Mach 4 combustion experiments as described in Sec. IV.A. This model calculated the experiment gas temperature using the combustor external outer wall temperature, measured using pyrometers positioned at irregular intervals axially along the combustor length and at two circumferential positions, both inline and between the injector locations. The analysis showed a sharp increase in gas temperature at approximately $x = 0.22$ m, indicating that combustion was initiated at this location. By starting the SHyFE vehicle during flight thermal modeling at 0.3 m it could therefore be assumed that the flame front had spread across the combustion chamber, allowing the gas across the combustion chamber height to be modeled as uniform. Figure 4 also shows that, once combustion was initiated, the gas temperature in the Mach 4 experiments remained approximately constant along the combustion chamber and that no variation in gas temperature was seen between the circumferential locations. It was, therefore, also appropriate to assume a uniform gas temperature axially and circumferentially in the SHyFE during the flight model combustion chamber.

The gas properties for the combustion section of the SHyFE during flight thermal model were set equal to the combustor exit gas properties calculated using the QinetiQ trajectory code created for the whole of the SHyFE acceleration period. The external air properties were also obtained from this code and held constant along the length of the vehicle.

To calculate the gas properties through the SHyFE nozzle, inviscid isentropic expansion equations were used to calculate the Mach number and area of the flow at 0.5 K static temperature T intervals between 500 K and the combustor exit total gas temperature (T_{0g}). The C_p and enthalpy h were calculated using a QinetiQ code containing empirical equations for an ideal gas, based only on T [6]. To convert the freestream gas properties to reference properties, the reference enthalpy was calculated using the Eckert method and Eq. (2) [7]. The external air heat transfer coefficient H was calculated using the Stanton number St_{air} equation for turbulent external flows along a flat plate [Eq. (3)] [7] with the boundary layer assumed to start adjacent to the combustor entrance along the SHyFE cowl ($x = 0$).

$$h^* = h + 0.5(h_{0g} - h) + 0.22(h_{\text{aw}} - h) \tag{2}$$

$$St_{\text{air}} = 0.0296\left(Re_x^{*-0.2}\right)Pr^{-2/3} \tag{3}$$

To account for the variation in geometry and surface temperature along the SHyFE combustion chamber and nozzle, the internal gas boundary layer St_g was calculated using Eq. (4). This equation is for a turbulent boundary layer with arbitrarily varying freestream velocity, density, and surface temperature [8] and the integration in the equation was performed using Simpson's rule.

$$St_g = 0.0287 Pr^{-0.4} \frac{rx^{0.25}\mu^{0.2}(T_{aw} - T^*)^{0.25}}{[\int_0^x rx^{1.25}\rho_\infty U_\infty, \mathrm{d}x(T_{aw} - T^*)^{1.25}]^{0.2}} \quad (4)$$

MATLAB[‡] was used to perform these calculations and construct a matrix containing the gas properties at each static temperature. This matrix was then interpolated using the area of the SHyFE nozzle at the axial locations specified by the thermal model to obtain the associated gas properties.

2. Thermal Resistance Equations

The thermal model represented each layer of the experimental cross section as a resistance, so the temperatures through the section were related to the adjacent surface by a single equation. From the known internal gas and external air temperatures for each short section, the code iterated to find the series of temperatures that made the net radial heat flow from the combustion gases into each section equal the net heat entering the fuel tank wall and radiating to the atmosphere.

The internal heat transfer coefficient H correlation allowed for the annular shape of the combustion chamber, leading to different H values for the inner and outer radii of each layer. Equation (5) shows the general resistance equation used to calculate the convective heat flow into and out of the discrete sections of the model. To account for the variation in the cross sectional areas through the SHyFE vehicle, the length ℓ of each section, in addition to the circumference C at the appropriate x location along the nozzle was included in the resistance equations. This converted heat flux to a heat transfer rate into each short section of combustion chamber or nozzle.

$$Q_{conv} = R_{conv}(T_{hot} - T_{cold}) \quad \text{where } R_{conv} = C \cdot H \cdot \ell \quad (5)$$

The radiation resistance was calculated using Eq. (6) [9], which models the radiation transfer between the two gray surfaces of concentric annuli by taking into account the difference in radii r and emissivity ε of the surfaces. Equation (7) [10] was used to calculate the radial heat transfer conducted through the annulus.

$$Q_{rad} = \sigma \cdot R_{rad}\left(T_{hot}^4 - T_{cold}^4\right) \quad \text{where } R_{rad} = \frac{C \cdot \ell}{\frac{1}{\varepsilon i} + \frac{1-\varepsilon o}{\varepsilon o}\left(\frac{r_i}{r_o}\right)} \quad (6)$$

$$Q_{cond} = R_{cond}(T_{hot} - T_{cold}) \quad \text{where } R_{cond} = \frac{2 \cdot \pi \cdot k \cdot \ell}{\ell_n\left(\frac{r_o}{r_i}\right)} \quad (7)$$

The resistance network used to construct the flight thermal model for each discrete 0.0007 m section is shown in Fig. 5

3. Heat Flow Balance Iteration

The iteration started at $x = 0.3$ m, where an initial guess was provided for the inner T_i and outer T_o wall temperatures. The iteration procedure then revised these temperatures to achieve a heat balance. As an example, the radial Q_{net} into the inner wall was calculated using Eq. (8). Once the heat flow model was assembled in Simulink,[§] iterative procedures were used to determine the unknown nozzle wall temperatures.

$$Q_{net,i,radial} = Q_{conv,i} + Q_{rad,i} = R_{conv,i}(T_g - T_i) + \left[R_{rad,i}\sigma\left(T_i^4 - T_o^4\right)\right] \quad (8)$$

Axial conduction was included in the thermal model by nesting the radial heat balance iteration within a second iteration loop. The Q_{net} equations were adjusted to include Q_{axial}, as illustrated by Eq. (9),

[‡]Matlab 6.5 release 13, The MathWorks, Ltd., Matrix House, Cambridge Business Park, Cambridge, CB4 0HH, England, www.mathworks.co.uk [retrieved 29 May 2007].

[§]Simulink 5.0 release 13, The MathWorks, Ltd., Matrix House, Cambridge Business Park, Cambridge, CB4 0HH, England, www.mathworks.co.uk [retrieved 29 May 2007].

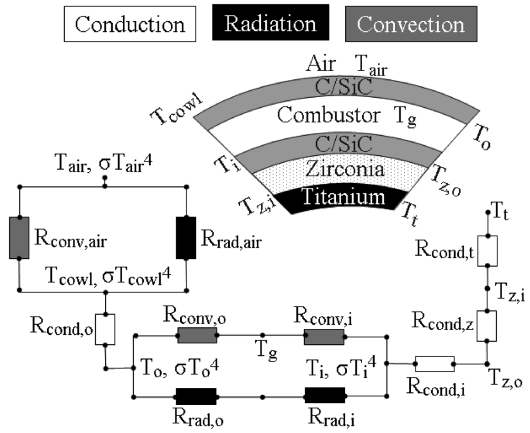

Fig. 5 SHyFE combustion chamber and nozzle during flight thermal model resistance network.

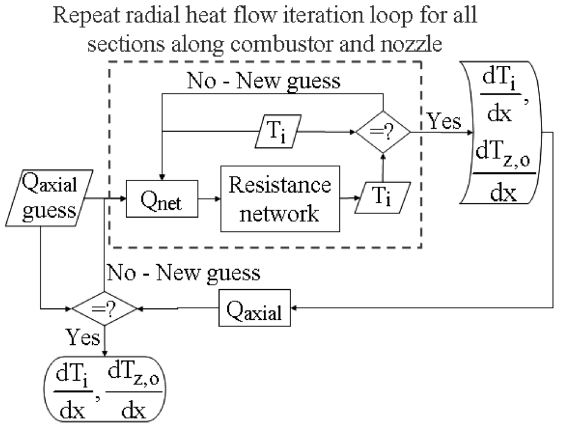

Fig. 6 Summary of SHyFE thermal model iteration loop for the inner combustor and nozzle walls.

which shows the inner wall Q_{net}. The radial heat flow balance was first performed iteratively to determine the inner and outer combustor and nozzle wall temperatures. This provided the temperature profile along the combustor and nozzle walls, allowing Q_{axial} to be calculated and fed back into the radial heat flow balance calculation. Figure 6 summarizes the iteration procedure.

$$Q_{net,i} = Q_{conv,i} + Q_{rad,i} - \left[\pi\left(r_{z,o}^2 - r_i^2\right)k\ell\frac{d^2\left(\frac{T_i + T_{z,o}}{2}\right)}{dx^2}\right] \quad (9)$$

IV. Thermal Model Validation

The SHyFE thermal model for flight was validated using gas and outer combustor wall temperatures measured at the combustor exit during Mach 4 combustion ground experiments. A regression procedure was used to select a combustion temperature that led to the modeled combustor external outer wall temperature $T_{j,air,i}$ matching the measured pyrometer temperature. Once $T_{j,air,i}$ had been matched to the experiment value, the predicted and measured combustor exit gas temperatures were compared to validate the thermal model.

A. SHyFE Mach 4 Combustion Experiments

1. Configurations

As prime contractor for SHyFE, QinetiQ assessed the combustion chamber and nozzle designs using two ground based experiments. These experiments tested full scale replicas of the SHyFE combustion chamber and nozzle and were carried out by QinetiQ staff in the QinetiQ combustion experimental rig. The air supplied to the combustor inlet was at the same conditions as predicted for the SHyFE flight vehicle during Mach 4 flight and fuel was sprayed into the combustion chamber using pressure swirl atomizers. This

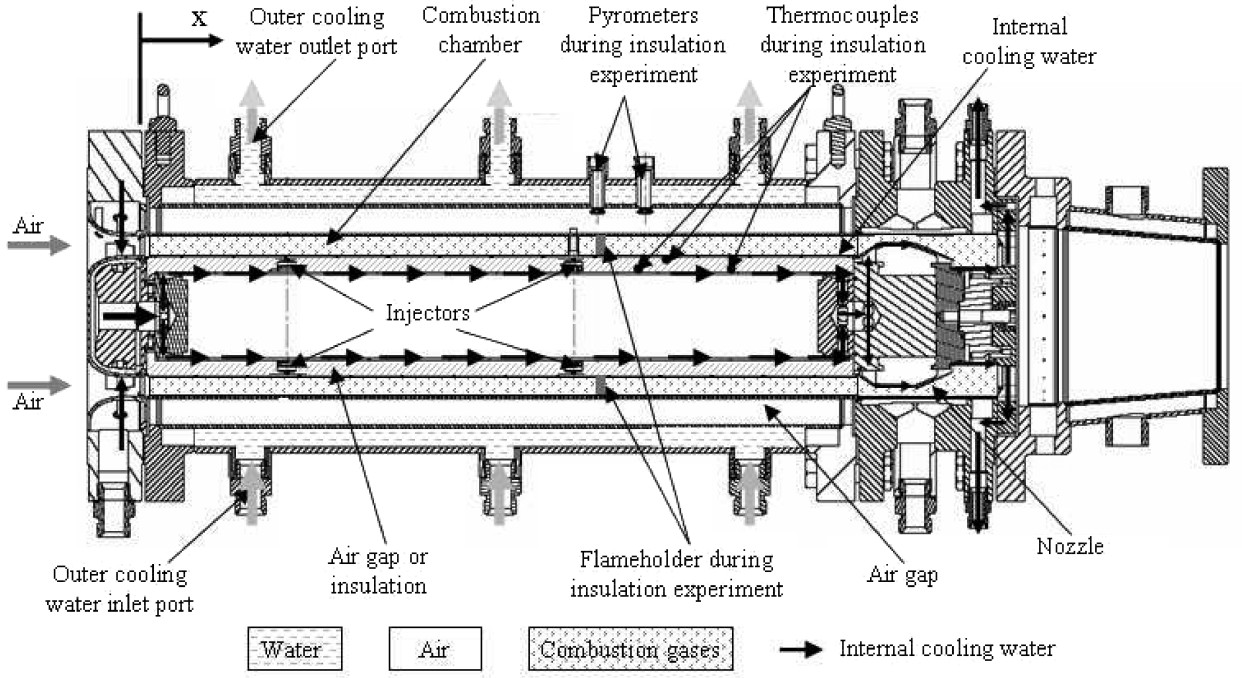

Fig. 7 Cross section through SHyFE Mach 4 combustion experiment.

configuration allowed the fuel ignition and thrust produced by the system to be measured at the same conditions as the start of the SHyFE acceleration.

To reduce the cost and risk associated with the preliminary evaluation of the SHyFE combustion process, both Mach 4 combustion experiments used a stainless-steel nozzle instead of the costly C/SiC nozzle intended for flight. The experiment was also initially run with an air gap between the inner combustor wall and the centerbody. A second set of experiments were then carried out with zirconia insulation located in this air gap.

Because of the external air remaining stationary during both tests and the use of stainless steel for the nozzle section, it was necessary to employ a cooling system in the experimental rigs. The cooling was provided using an external water cooled jacket and a complex series of water channels along the internal surfaces of the combustion chamber and nozzle, as shown in Fig. 7.

Water was supplied to the internal cooling system through six struts within the intake of the test section and flowed around the inside of the intake cone to the center of the test rig. The internal cooling water was then channeled downstream and delivered into a very thin annulus between the internal air gap and the experiment centerbody. The same cooling water finally passed directly below the inner wall of the stainless-steel nozzle before being ejected through six struts in the exhaust of the experimental configuration. Ports in the top and bottom of the apparatus allowed 15.2 $kg \cdot s^{-1}$ of water to flow around the outside of the combustor and nozzle, while 4.7 $kg \cdot s^{-1}$ of water was passed internally along the entire length of the experimental configuration. The internal and external water mass flow rates were fixed by the cooling water available to the QinetiQ combustion rig. The convective heat transfer rate to the experiment cooling water therefore did not match the predicted total heat transfer rate to the external air for the SHyFE vehicle during the Mach 4 flight.

To improve the combustion efficiency of the SHyFE vehicle, the flameholder shown in Fig. 8 was introduced into the C/SiC combustion chamber during the zirconia insulation set of Mach 4 combustion experiments. The flameholder was located 50 mm downstream of the rear injector location, as shown in Fig. 7.

2. *Temperature Measurement*

The nozzle temperature was measured by QinetiQ during the air gap combustion chamber experiment using thermocouples sprung loaded against both the inner and outer combustor tubes [3]. However, the outer combustor tube thermocouples were found to be in poor contact during the experiments, resulting in erroneous readings during the zirconia insulation Mach 4 combustion experiments. The thermocouples on the outer combustor tube were therefore replaced by QinetiQ with 16 noncontact infrared temperature sensors. Each pyrometer was positioned so that it viewed the external outer combustor surface through a tube in the outer cooling water jacket, as shown in Fig. 7. To calculate the temperature of the inner tube, the emissivity of the C/SiC was assumed to be 0.85 [3].

The combustor exit gas temperature was calculated during the Mach 4 combustion experiments by calculating the characteristic velocity C^*, defined in Eq. (10) [11]. The total pressure at the entrance to the nozzle $P_{0,c,\text{exit}}$, the throat area A^*, and total mass flow rate were measured during the Mach 4 combustion experiments and therefore C^* could be calculated during SHyFE ground experiments.

$$C^* = \frac{P_{0,c,\text{exit}} A^*}{\dot{m}_{\text{air}} + \dot{m}_f} \tag{10}$$

The total mass flow rate $(\dot{m}_a + \dot{m}_f)$ through the SHyFE nozzle can be written as Eq. (11) if the flow is assumed to be isentropic and calorically perfect and the nozzle choked. In this case C^* can be written as Eq. (12), which can be rearranged to allow $T_{0,c,\text{exit}}$ to be calculated [12]. The combustion gas specific heat ratio γ, and molecular mass (required to calculate the correct gas constant Rc) were calculated using Gordon and McBride's chemical equilibrium analysis program [13]. This program predicted the equilibrium conditions of reacting gases after isentropic expansion through the

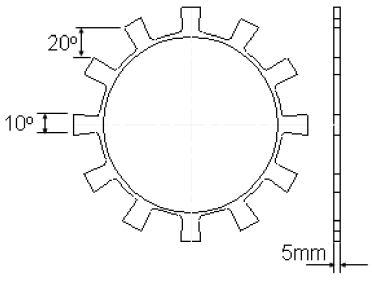

Fig. 8 Low blockage thin ring flameholder used during Mach 4 zirconia insulation combustion experiment.

SHyFE Mach 4 combustion experiment pressure and area ratio.

$$\dot{m}_{\text{air}} + \dot{m}_f = \frac{P_{0,c,\text{exit}} A^*}{\sqrt{T_{g,\text{exit}}}} \sqrt{\frac{\gamma}{R}\left(\frac{2}{\gamma+1}\right)^{(\gamma+1)/(\gamma-1)}} \tag{11}$$

$$C^* = \frac{\sqrt{\gamma R_c T_{g,\text{exit}}}}{\gamma\sqrt{[2/(\gamma+1)]^{(\gamma+1)/(\gamma-1)}}} \tag{12}$$

B. Thermal Modeling of the SHyFE Mach 4 Combustion Experiments

The thermal models of the SHyFE Mach 4 combustion experiments were based on the thermal model for the SHyFE combustion chamber and nozzle during flight. The combustion chamber and nozzle were again split into short lengths, over which the experiment surface and gas temperatures were assumed to be uniform. The surface temperatures along each short section were calculated using the same iterative procedure as the flight model. The nozzle and combustor temperatures were, however, only calculated for a single flight speed and therefore the combustion chamber and nozzle gas properties only varied with x location. The Mach 4 combustion experiment thermal models used the same resistance equations and heat balance approach as the nozzle during flight thermal model, however, the experiment geometries led to slight alterations in the resistance networks.

Figures 9–11 show the Mach 4 combustion experiment geometries in addition to the nomenclature for the resistance networks used in the thermal models. The combustor and nozzle gas H values were calculated using the same equations as those used in the flight thermal model.

A series of heat transfer coefficient experiments, carried out by the authors and detailed in [14] showed that introducing the flameholder into the SHyFE combustion chamber at Mach 4 flight conditions raised the combustion gas Stanton number by a factor of 2 at the combustor exit compared to the undisturbed flow value. This factor was included in the combustion experiment thermal model.

The heat balance iteration loop was performed in exactly the same way as the SHyFE during flight thermal model. Starting at the inlet to the combustor, the heat flow from the combustion gases for each short section was calculated. The adjacent downstream combustion gas and nozzle cooling water temperatures were then determined using Eq. (13). By assuming that T_g stayed constant along the length of the combustion chamber, the thermal model was able to step along

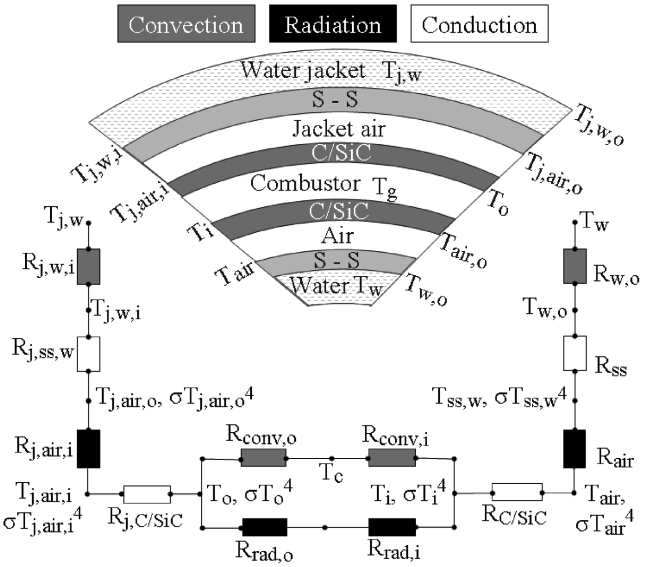

Fig. 9 Mach 4 combustor experiment containing an air gap between the combustion chamber centerbody. Used for internal cooling water system design thermal model.

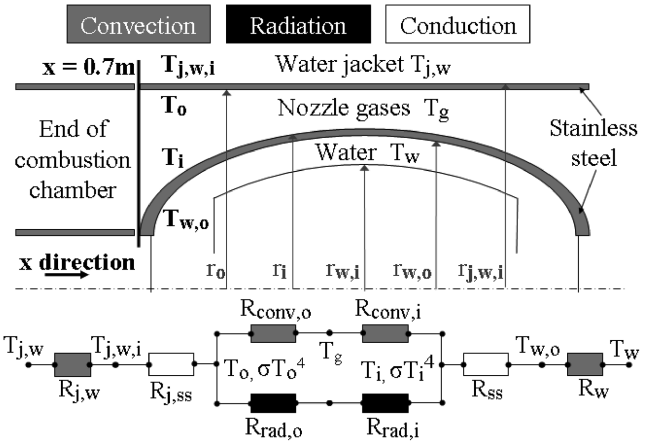

Fig. 10 Mach 4 combustion experiment nozzle geometry, nomenclature, and thermal model resistance network.

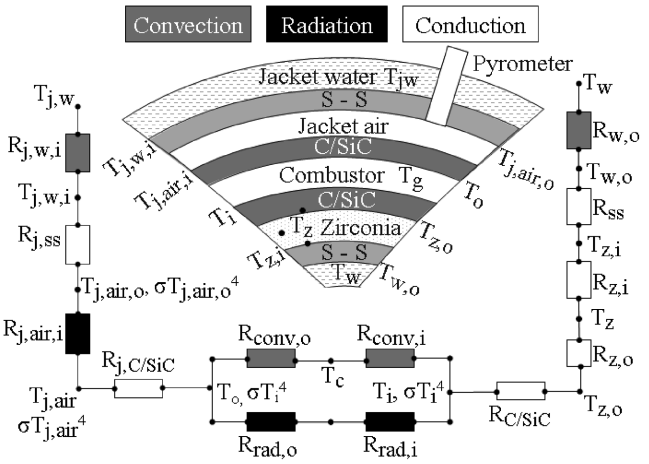

Fig. 11 Thermocouple validation thermal model nomenclature and resistances.

the length of the experiment, repeating the heat balance iteration until a complete analysis of the temperatures through and along the SHyFE Mach 4 combustion experiment was completed. $T_{w,\text{DS}}$ and $T_{w,\text{US}}$ indicate the downstream and upstream section cooling water temperatures, respectively, and $\dot{m}_w$ and $C_{p,w}$ are the values of mass flow rate and specific heat for the cooling water.

$$T_{w,\text{DS}} = T_{w,\text{US}} + \frac{Q_{\text{net}}}{\dot{m}_w \cdot C_{p,w}} \tag{13}$$

C. Validation Methodology and Results

The outer combustor wall pyrometer temperature measurements obtained by QinetiQ during the zirconia insulation Mach 4 combustion experiments allowed the thermal models to be validated. The thermal model was used to calculate the gas temperatures during the experiment when combustion was undertaken at equivalence ratios of 0.79 and 0.86. The pyrometer temperature measurements were performed at a number of locations along the combustion chamber, including one close to the combustor exit. It was therefore possible to run the Mach 4 combustion experiment thermal model at a range of combustion gas temperatures, until the outer tube external surface temperature $T_{j,\text{air},i}$ matched the measured value at the pyrometer location. The thermal model combustion gas temperature was then compared with the measured combustor exit gas temperature, calculated from the C^* parameter (Sec. IV.A).

Figure 12 shows the thermal model gas temperature prediction against the gas temperatures measured using the C^* parameter. A false zero is used on the value axes to aid the comparison between the thermal model, and the uncertainties in the modeled combustor exit

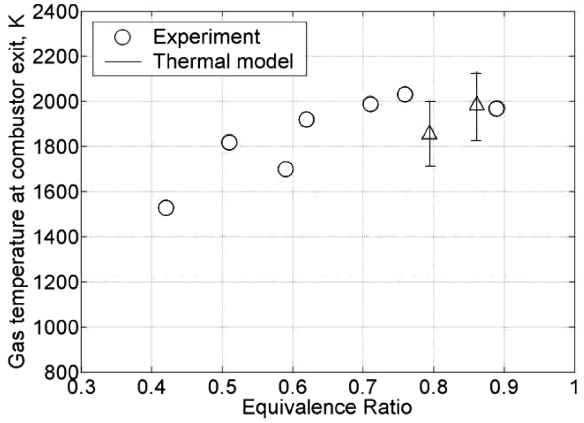

Fig. 12 Comparison between zirconia insulation SHyFE Mach 4 experiment and thermal model combustor exit gas temperature.

gas temperatures are also shown. Estimates of the T_g uncertainty have been made using the method of small perturbations described by [15] and shown in Table 1. A worst case uncertainty of 8.8% was calculated by assessing the sensitivity of the thermal model results to uncertainties in the C/SiC conductivity k and emissivity ε values, in addition to uncertainty associated with parameters obtained from experimental measurements. The SHyFE Mach 4 combustion experiment provided the air mass flow rate $\dot{m}_{\text{air}}$, and outer combustor wall $T_{j,\text{air},i}$ temperature measurements. The accuracy of the $\dot{m}_{\text{air}}$ measurements was assumed to be $\pm 1\%$ and the $T_{j,\text{air},i}$ uncertainty was calculated as $\pm 5.7\%$ by combining the pyrometer measurement uncertainties. The pyrometer measurement uncertainties consisted of the pyrometer sensitivity, which was quoted by the manufacturer as $\pm 1\%$ and the C/SiC ε error, which QinetiQ stated as ± 0.05. The Stanton number was influenced by the thermochromic liquid crystal uncertainty associated with experiments carried out by the authors [4] to assess the Stanton number increase downstream of the flameholder. The value quoted for C/SiC thermal conductivity k varies depending on the source consulted [3,5] and therefore a $\pm 1\ \text{W} \cdot \text{m}^{-1} \cdot \text{K}^{-1}$ uncertainty was used. The uncertainty in the C/SiC ε was also included in the total thermal model gas temperature uncertainty, to account for its use within the thermal model radiation calculations.

Taking the thermal model experiment uncertainties into account, the thermal model combustor gas exit temperatures lie within -9% and $+15\%$ of the experimental data at the 0.79 and 0.86 equivalence ratios. This provides confidence that the thermal model methodology is suitable for predicting the temperatures through the SHyFE vehicle and that predictions of the SHyFE wall temperatures throughout the acceleration portion of the SHyFE mission are valid.

V. Use of the SHyFE Mach 4 Combustion Experiment Thermal Models

In addition to validating the SHyFE during flight thermal model, the Mach 4 combustion experiment thermal models were used to aid the design of the experiment cooling water system and to assess the validity of the zirconia insulation combustion chamber thermocouple measurements.

Table 1 Contributions to uncertainties in thermal model combustor exit gas temperature predictions

Test condition	Typical value	Typical uncertainty	T_g error, %
$T_{j,\text{air},i}$, K	1642	± 93	7.6
Stanton no.	1.4	± 0.11	-0.8
k C/SiC, $\text{W} \cdot \text{m}^{-1} \cdot \text{K}^{-1}$	18	± 1	0.0
ε	0.85	± 0.05	0.3
$\dot{m}_{\text{air}}$, $\text{kg} \cdot \text{s}^{-1}$	1.544	± 0.0154	-0.1
——	Thermal model T_g value, K		1858
——	Root sum square error, %		7.7
——	Maximum error, %		8.8

A. Internal Cooling Water System Design Improvements

During the design phase of the SHyFE Mach 4 combustion experiments, the thermal model containing an air gap between the combustion chamber and centerbody was used to ensure that the internal cooling water system was capable of removing sufficient heat from the experimental configuration. The temperature of the nozzle was calculated with the cooling water annulus height initially set to 2 mm. This showed that the surface temperatures through the nozzle section were below the stainless-steel thermal limits, but that the stainless-steel surface temperature adjacent to the internal cooling water annulus $T_{w,o}$ was over 100 K greater than the boiling temperature of water at the pressures anticipated in the nozzle cooling water annulus. This meant that the water at this location was unlikely to provide adequate cooling. The geometry was changed and the thermal model rerun with a 1 mm nozzle internal cooling water annulus height. This increased the velocity of the water through the internal cooling water channel, reducing the stainless-steel temperature next to the internal cooling water to below the boiling temperature of the water.

B. Thermocouple Validation

On completion of the zirconia insulation combustor tests it was necessary to assess the validity of the thermocouple measurements. The authors therefore used the Mach 4 combustion experiment thermal model to predict the temperatures through the insulation, so that the predicted and experiment thermocouple temperatures could be compared.

The thermocouples were placed at a range of depths into the zirconia insulation between the combustion chamber and centerbody, as shown in Fig. 7. To predict the thermocouple temperatures, each thermocouple position was paired with an external outer combustor wall temperature $T_{j,\text{air},i}$ at the same x location, obtained through linear interpolation of the pyrometer measurements. The zirconia insulation was modeled using two adjacent conduction resistance equations ($R_{z,i}$ and $R_{z,0}$), described by Eq. (7). The thermocouple temperature was calculated as the temperature at the junction of the two zirconia conduction resistance equations T_z. This method allowed the depth of the thermocouples to be varied by changing the inner and outer radii in the conduction resistance equations.

The thermocouple temperatures were predicted using the same method as the nozzle during flight thermal model validation. For each thermocouple the model was run at a range of combustion gas temperatures until the outer wall external surface temperature $T_{j,\text{air},i}$ matched the temperature measured by the pyrometer. At locations downstream of the flameholder, the combustion gas St_g values were factored to account for the flameholder in the combustion chamber. The factor values were measured during the heat transfer experiments presented by the authors in [4]. These experiments provided the average St_g at 4 mm intervals along the combustor, allowing the St_g increase downstream of the flameholder to be obtained for each of the thermocouple x locations.

Figure 13 shows that the model thermocouple T_z and gas temperatures T_g follow the pyrometer external outer combustor wall $T_{j,\text{air},i}$ trend. The measured T_z values do not follow this trend, however, leading to the conclusion that the thermocouples did detach from the inner combustor wall during the Mach 4 combustion experiment.

C. SHyFE Combustion Chamber and Nozzle During Flight Thermal Model Results

1. *Temperature and Heat Flow Predictions*

Figures 14a and 14b show the internal inner and outer combustion chamber and nozzle wall temperatures at a range of times during the acceleration section of the SHyFE flight, without the flameholder located in the combustion chamber. This shows that the highest

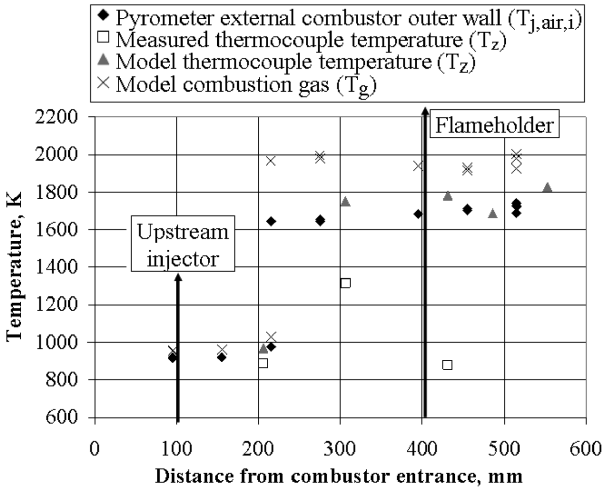

Fig. 13 Measured and model combustor wall T_z and $T_{j,\mathrm{air},i}$ and gas T_g temperatures. Note that the model combustor external outer wall temperatures (not shown) were matched to the pyrometer data.

temperatures are predicted to occur just downstream of the nozzle. This is to be expected, as the exhaust gas velocity is highest at this location leading to the largest values of H and therefore the maximum convective heat transfer to the nozzle walls.

Figures 15a and 15b show the nozzle throat heat flow throughout the SHyFE acceleration, illustrating that the maximum heat transfer rate occurs 7 s after the start of the SHyFE acceleration. The net heat transfer rate is governed by the combustor internal wall H values, which are largely influenced by the product of the combustion gas density and velocity. As the SHyFE vehicle accelerates and gains altitude, the gas density decreases, but the velocity increases, leading to the variation in mass flow rate shown in Fig. 15c. Up to 7 s the increased velocity is dominant, leading to $\dot{m}$ getting larger, however, the reduction in density with altitude becomes dominant at 7 s and $\dot{m}$ reduces beyond this time.

Figure 16a shows that the outer tube throat temperature drops between 0 and 3 s and then peaks at 4 s, before cooling during the remainder of the SHyFE acceleration. The reason for this irregular outer wall temperature change at the beginning of the SHyFE acceleration can be seen in Fig. 16b, which shows that the difference between the external and internal SHyFE surface boundary layers leads to the external H value increasing much more rapidly than the internal H.

The convection heat transfer is much larger than the radiation heat transfer, both inside the combustion chamber and outside the cowl, leading to H governing the heat flow and therefore temperatures of the SHyFE walls. The rapid external H increase, compared to the near constant internal outer wall H, causes the surface of the C/SiC adjacent to the atmosphere to begin cooling at the start of the acceleration. At $t = 4$ s, however, the internal outer wall H increases and reduces the gap between the external and internal outer wall heat flows, so that the outer wall temperature increases. Beyond 7 s, the heat transfer to the inner wall reduces, while the external heat transfer increases. This leads to a reduction in the outer wall temperature throughout the rest of the SHyFE flight, despite the reduction in external heat flow from 12 s onward.

Figure 16c shows that the maximum inner wall temperature occurs 7 s after the start of the SHyFE acceleration. The radiation increase from the inner combustor and nozzle walls as the outer tube cools down is not great enough to counteract the increased internal convection heat transfer, leading to the inner tube temperature initially increasing during the SHyFE flight. When the net heat transfer to the inner combustor and nozzle wall reduces after 7 s, however, the temperature of the inner combustor and nozzle surfaces is predicted to reduce.

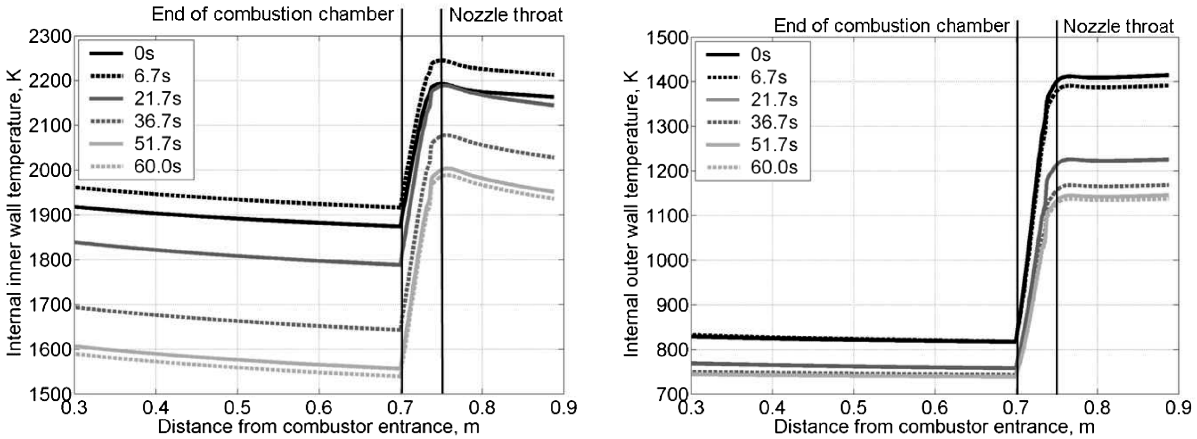

a) Inner wall **b) Outer wall**

Fig. 14 Internal wall temperature T_i and T_o variation with time and distance along the SHyFE vehicle.

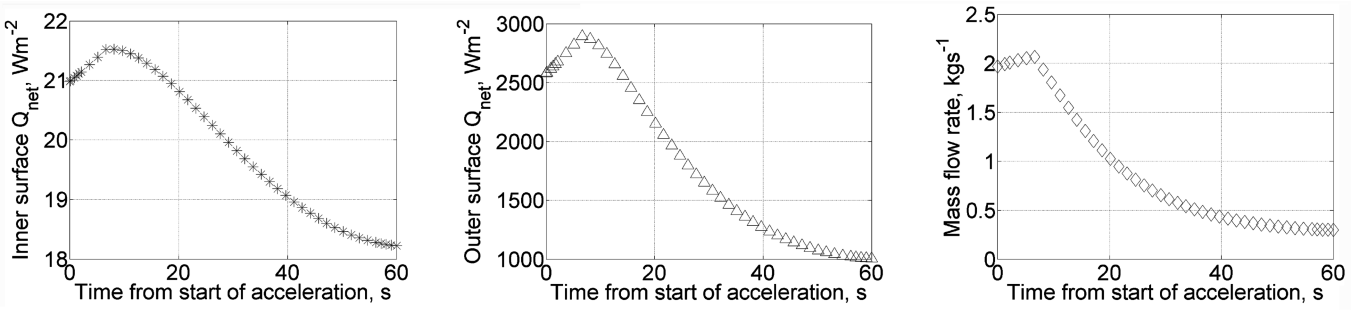

a) Inner wall heat flow **b) Outer wall heat flow** **c) Combustion gas mass flow rate**

Fig. 15 SHyFE heat and mass flow rate variation at throat location during acceleration.

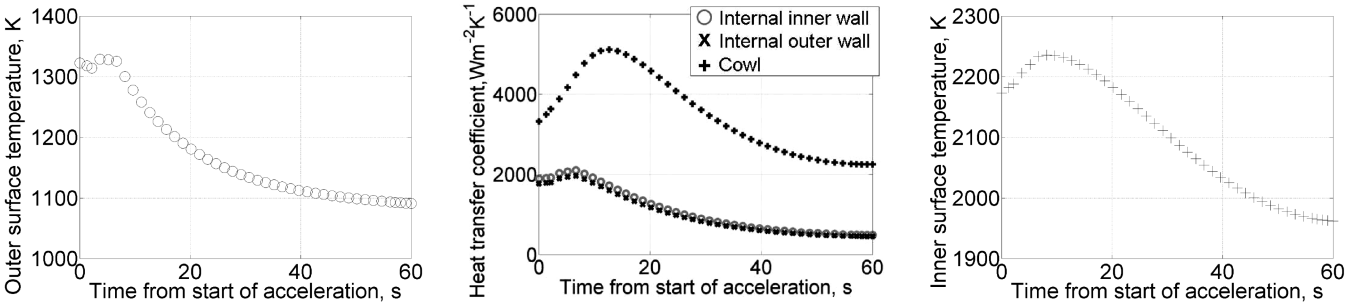

a) Outer wall temperature b) Heat transfer coefficient c) Inner wall temperature

Fig. 16 SHyFE temperature and heat transfer coefficient variation at throat location during acceleration.

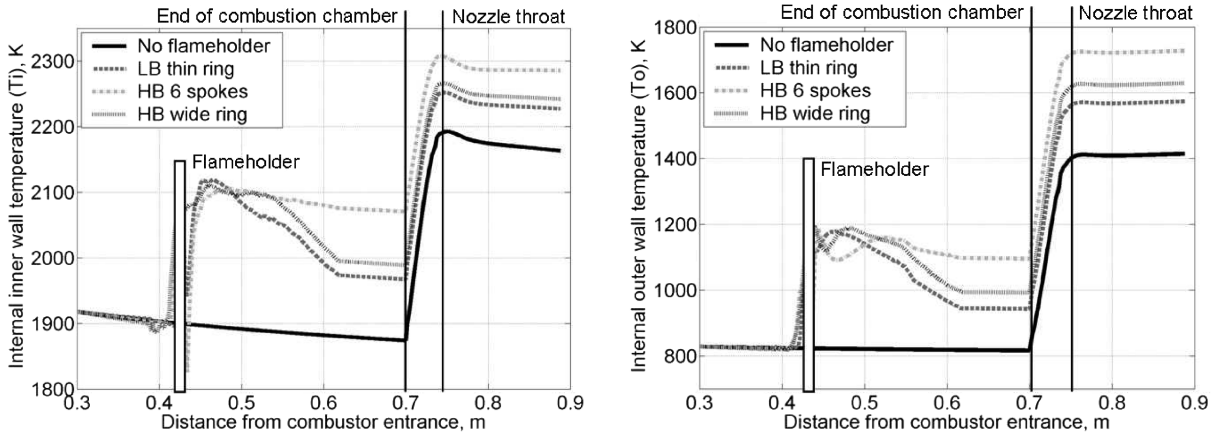

a) Inner wall b) Outer wall

Fig. 17 Mach 4 flight SHyFE wall temperatures with and without flameholder located in combustion chamber. HB stands for high blockage and LB for low blockage.

The nozzle wall temperatures are shown to stay below the C/SiC temperature limits throughout the acceleration section of the flight. The maximum heat flow during the acceleration period was also calculated, showing that the fuel temperature is expected to rise by only 1°C during the acceleration period, giving a fuel temperature which is well below the autoignition temperature of the diesel and a payload temperature below the thermal limit of the flight control actuators and computer.

2. *Flameholder Analysis*

The combustion chamber and nozzle flight thermal model was also used to help assess the suitability of a range of flameholder designs for the SHyFE vehicle. The flameholder designs were assessed using experiments and computational fluid dynamics detailed in [4]. These analyzed the influence of spoke width, blockage ratio, ring position, and ring shape on the combustion mixing efficiency and H increase through the SHyFE combustion chamber and nozzle.

The flameholders increase the SHyFE internal wall H values by introducing high levels of recirculation downstream of the spokes, causing the flow to separate and reattachment over the flameholder rings and by causing high velocity jets to form between the flameholder spokes. The thermal model was used to assess the influence that the H increase, induced by the flameholder designs, would have on the temperature of the SHyFE vehicle walls. This was achieved by dividing the Stanton number values measured along the length of the flameholder experiments by the Stanton number values measured without the flameholder in place. The Stanton number values in the thermal model were then multiplied by this factor.

Figures 17a and 17b show the nozzle wall temperature predictions for the flameholder designs shown in Figs. 8, 18, and 19, at the start of the SHyFE acceleration. It can be seen that the C/SiC nozzle inner wall throat temperature downstream of the 6-spoke flameholder design reaches the 2300 K thermal limit of the C/SiC. The wall temperatures downstream of all the other flameholders are, however, within the temperature capabilities of the C/SiC.

VI. Conclusions

A steady-state thermal resistance network thermal model has been used to predict the surface temperatures and heat flow in the SHyFE combustion chamber and nozzle during the acceleration section of the flight experiment. This has shown that the maximum heat flows

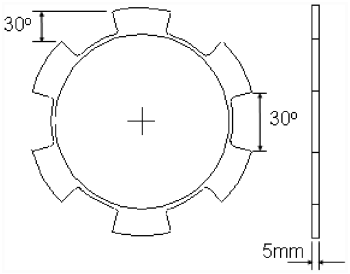

Fig. 18 High blockage 6-spokes flameholder.

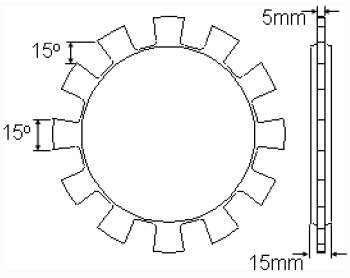

Fig. 19 High blockage wide ring flameholder.

are predicted to occur at the throat position, approximately 7 s after the start of the acceleration. The maximum wall temperatures are also predicted to occur at the nozzle throat, approximately 7 s after the start of the acceleration.

The flexibility of the thermal model has enabled the resistance network methodology to be easily altered to predict the temperatures through SHyFE Mach 4 combustion experiments. The modular design of the thermal model has allowed an air gap or zirconia insulation to be incorporated into the model between the internal combustor wall and the centerbody.

The Mach 4 combustion experiment modeling was used to validate the thermal model methodology by predicting combustor exit gas temperatures close to the experimental measurements. The thermal model was also used to check thermocouple measurements during the Mach 4 SHyFE combustor experiments.

The ease with which the thermal model can be reconfigured made it highly suitable for the thermal design of the SHyFE Mach 4 combustion experiment cooling water system. The model highlighted the need to alter the internal cooling water annulus adjacent to the stainless-steel SHyFE nozzle and allowed the authors to specify the most appropriate height for the cooling water channel.

The SHyFE flight model has been used to assess the temperature and heat flows associated with a range of flameholders during the SHyFE flight experiment. This investigation concluded that only the 6-spoke flameholder design would induce inner tube temperatures above the C/SiC thermal limit, with the other flameholder designs inducing lower nozzle temperatures.

The resistance modeling methodology described in this paper can be used for any subsonic thermal system where the time period of interest is long enough that steady-state analysis can be used. Detailed knowledge of the system geometry is not required and temperature and heat flows can be quickly calculated in the time and two-dimensional space domains without the need for finite element modeling. The driving gas temperature must be known throughout the time period of interest, in addition to the external air temperature. Geometry alterations can, however, be easily incorporated into the model by altering and introducing additional resistance equations.

Acknowledgments

The authors gratefully acknowledge the U.K. Ministry of Defence Weapon Effectors and Equipment (WPE) domain for financially supporting this project. J. S. Goodman was partly funded by the Engineering and Physical Science Research Council and the Jesus College Old Members' Group 1969–64. The authors are very grateful for the expert guidance from QinetiQ, as prime contractor for the work.

References

[1] Cain, T., and Walton, C., "The Sustained Hypersonic Flight Experiment," AIAA Paper 2003-7030, 2003.

[2] Handrick, K., "Space Products and High Tech Ceramics, MAN Technologie AG, Augsburg, Germany, Nov. 2004.

[3] Cain, T., and Walton, C., "SHyFE Phase 1 Final Report," QinetiQ, QINE-TIQ/FST/WNS/CR051184, Farnborough U.K., March 2005.

[4] Goodman, J. S., and Ireland, P. T., "Heat Transfer and Flow Investigation of a Multi-Spoke Flameholder for an Annular Combustor," *Proceedings of the Fifth International Symposium on Turbulence Heat and Mass Transfer*, International Centre for Heat and Mass Transfer, Ankara, Turkey, 2006, pp. 731–734; also THMT Paper 06/28.1.

[5] Brandt, R., Frieß, M., and Neuer, G., "Thermal Conductivity, Specific Heat Capacity and Emissivity of Ceramic Matrix Composites at High Temperatures," *High Temperatures—High Pressures*, Vols. 35/36, 2003/2004, pp. 169–177.

[6] Van Wylen, G. J., and Sonntag, R. E., *Fundamentals of Classical Thermodynamics*, 2nd ed., Wiley, New York, 1978, pp. 683–684.

[7] Kays, W. M., and Crawford, M. E., *Convective Heat and Mass Transfer*, 3rd ed., McGraw–Hill, New York, 1993, pp. 271–293.

[8] Kays, W. M., and Crawford, M. E., *Convective Heat and Mass Transfer*, 3rd ed., McGraw–Hill, New York, 1993, pp. 233–255.

[9] Incropera, F. P., and DeWitt, D. P., *Introduction to Heat Transfer*, 4th ed., Wiley, New York, 2002, pp. 748–816.

[10] Incropera, F. P., and DeWitt, D. P., *Introduction to Heat Transfer*, 4th ed., Wiley, New York, 2002, pp. 87–182.

[11] Sutton, G. P., and Biblarz, O., *Rocket Propulsion Elements*, 7th ed., Wiley-Interscience, Toronto, 2001, pp. 27–44.

[12] Sutton, G. P., and Biblarz, O., *Rocket Propulsion Elements*, 7th ed., Wiley-Interscience, Toronto, 2001, pp. 45–101.

[13] McBride, B. J., and Gordon, S., "Computer Program for Calculation of Complex Chemical Equilibrium Compositions and Applications," NASA RP-1311, June 1996.

[14] Goodman, J. S., "Thermal Design of Hypersonic Ramjets," D.Phil. Thesis, University of Oxford, Oxford, U.K., 2007.

[15] Moffat, R. J., "Contributions to the Theory of Single-Sample Uncertainty Analysis," *Journal of Fluids Engineering*, Vol. 104, June 1982, pp. 250–260.

[16] Cain, T., and Walton, C., "Sustained Hypersonic Flight Experiment First Year Review," QinetiQ, QINETIQ/FST/CDT/CR022294, Farnborough, U.K., April 2002.